International Communications in Heat and Mass Transfer 119 (2020) 104968

Contents lists available at ScienceDirect

International Communications in Heat and Mass Transfer

journal homepage: www.elsevier.com/locate/ichmt

Numerical and scale analysis of Eyring-Powell nanofluid towards a magnetized stretched Riga surface with entropy generation and internal resistance

Mubbashar Nazeer[a], M. Ijaz Khan[b], M. Usman Rafiq[b,c], Niaz Bahadur Khan[d,*]

[a] Department of Mathematics, Institute of Arts and Science, Government College University Faisalabad, Chiniot Campus, Pakistan
[b] Department of Mathematics and Statistics, Riphah International University I-14, 44000, Pakistan
[c] Department of Mathematics, Riphah International University Faisalabad Campus 38000, Pakistan
[d] Department of Mechanical Engineering, University of Malaya, Malaysia

ARTICLE INFO

Keywords:
Riga plate
Activation energy
Eyring-Powell fluid
Numerical method
Heat transfer rate

ABSTRACT

The aim of current investigation is to report the impact of convective boundary conditions, heat generation, viscous dissipation, porous medium and activation energy on Eyring-Powell nanofluid over Riga plate. We have used the Darcy-Forchheimer model to characterized the effects of porous medium. The Riga plate describes as an electromagnetics actuator that is made of permanent magnets and recurring behavior of electrodes pointed on plane of surface. Mathematical formulation is derived with viscous dissipation, heat generation and activation energy. The numerical code of shooting method is developed based on Range-Kutta Method of order four to get the fast convergence and accurate results. It is analyzed that the temperature field shows an increasing behavior by varying the values of Eckert number (*Ec*) radiation parameter (*Rd*). The Eckert number and modified Hartman number *Q* accelerate both velocity and temperature profiles, respectively. The nanoparticle concentration profile increases with Eckert number. The walls shear stress is increases and decreasing behavior for the values of modified Hartmann number and Eyring-powell parameter.

1. Introduction

Present study ensures that nanofluids have great importance in industrial and technological process. A fluid which contains the nano-sized particles (Nanoparticles) is called a nanofluid. The word Nano is derived from Latin word which means gnome. These nanoparticles are generally made of oxide ceramic-Al_2O_3, metal carbides-Sic, nitrides-ALN, SIN, metals-Al, Cu and nonmetals- Graphite, carbon nanotube. Its major use in pharmaceutical nanotechnology which is based on nano-size particles like polymer nanoparticles, magnetic nanoparticles, liposomes, carbon nanotube and metallic nanoparticles. These nanoparticles stay hanged for a long period of time in the base fluid. Choi [1] presented the nanofluid and described that nanofluids have great importance in medical field like healing of cut, unblocking/opening the vessels, hyperthermia etc., are completely dependent on the characteristics of nanofluids. Nanofluids are favorable in mass and heat transfer characteristics particularly in heat exchanger, aerospace technology, refrigeration and micro processing etc. Rasool et al. [2] reported that the nanoparticles can hanged in the fluid for a long period of time that have size less than 100 nano-meter and concluded that the velocity field of the nanofluid particles and the modified Hartman number have direct proportional relation. Buongiorno [3] used the concept of nanofluid and derived a mathematical model to observe the thermal applications of base fluids. The base of this model depend on two parameters, thermophoresis parameter (*Nt*) and Brownian motion parameter (*Nb*). Various investigations have been performed and available in the literature to report the applications of nanofluid in different geometries [4,5–10].

In branch of fluid mechanics, the magnetic field have great importance due to its different properties in augmentation of thermal-physical properties of a fluid. A magnetic field is a vector field that elaborates the magnetic effect of electric charges in relative motion and magnetized materials. It is used in electric motors, electric generators, electric transformers and magnetic resonance imaging (MRI). Waqas at el. [11] discussed the behavior of magnetic dipole and activation energy for nanofluid over the stretchable surface to identify the importance of fluid under the establishment of magnetic field. They also considered the Brownian and thermophoresis conditions of liquid and

* Corresponding author.
E-mail addresses: mubbasharnazeer@gcuf.edu.pk (M. Nazeer), n_bkhan@siswa.um.edu.my (N.B. Khan).

https://doi.org/10.1016/j.icheatmasstransfer.2020.104968

Nomenclature

$\widetilde{\mu}$	dynamic viscosity
$\widetilde{\rho}_l$	density of base fluid
$\widetilde{\nu}$	kinematic viscosity
$\widetilde{\gamma}$, $\widetilde{C}$	material constant
$\widetilde{\sigma}$	electric-conductivity
$\widetilde{\alpha}$	thermal diffusivity
$\widetilde{k}$	thermal conductivity
$(\widetilde{\rho}c)_p$	heat capacity of fluid
$\widetilde{D}_B$	Brownian motion
$\widetilde{D}_T$	thermophoresis diffusion
$\widetilde{T}_\infty$	temperature distribution
$\widetilde{C}_\infty$	concentration distribution
$\widetilde{J}_o$	density of applied current
$\widetilde{M}_o$	magnetization in magnet
$\widetilde{b}$	width of magnet and electrodes
$\widetilde{\tau}$	ratio between productivity of heat capacity of fluid and nanoparticles
$\widetilde{q}_r$	radiative heat flux

action of activation energy on the flow field. Lielausis and Gailities [12] firstly was made this type of development in Riga and assigned a name of Riga plate. The Riga plate describes as an electromagnetics actuator that is made of permanent magnets and recurring behavior of electrodes pointed on surface plane. Magyari et al. [13] described the inverse relation between the Hartman number and transverse velocity through the mixed convective flow over a Riga plate. Chamkha et al. [14] analyzed the Marangoni convection of nanofluid under the effect of Lorentz force. Balazadeh et al. [15] discussed the flow of non-Newtonian fluid through a Riga plates under the impact of magnetic field and joule heating.

In fluid mechanics, various types of the chemical reaction are happened in the complex system of fluids, such as: heterogeneous reactions and homogeneous reaction etc. Seyedi et al. [16] reported the applications of chemical reaction over a stretching wall under the consider of radiative heat flux. Viscoelastic fluid over a stretch sheet under the impact of homogeneous-heterogeneous reaction were numerically analyzed by Khan et al. [17]. Squeezed flow was considered by Hayat et a. [18] to highlight the impact of chemical reaction and convective conditions to report the importance of various physical parameters on the involving unknown physical quantities. Williamson nanofluid with variable thickness, thermal radiation, chemical reaction and Lorentz force was taken by Kumar et al. [19].

It is well-known that the Navier stokes equations cannot be support to understand the complex rheological fluids like, typical oil, human blood, polymer solution, various paints and grease etc. Because, in these fluid models, a highly nonlinear relation between shear stress and strain is observed. To understand the behavior of such type of fluids, various non-Newtonian models have been presented including Powell-Eyring fluid which is taken in this investigation. This fluid model product the non-Newtonian behvaiour at an intermediate stress rate and behave like viscous fluid against the highly shear stress rate. Moreover, this model is derived from the constitutive expression obtained by the kinetic theory of gases instead of empirical formula. This model has significant applications in industrial processes (polymer solution) and chemical engineering process. For this, Ali et al. [20] discussed the Powell-Eyring fluid through a pipe under the effects of variable liquid properties. They used the numerical and analytical techniques to handle the developed nonlinear system of equations. Alsaedi et al. [21] expressed the energy loss of thermodynamic system by using the stretchable surface in MHD Eyring-Powell nanofluid and explained the thermal conductivity of the system raised by using nanoparticles in the ordinary liquid. Nazeer et al. [22,23] analyzed the flow behavior of non-Newtonian fluid under the impact of space and temperature dependent viscosity models. Recently, Khan et al. [24] investigated impact of modified homogeneous-heterogeneous reactions in flow of Casson liquid towards a stretched surface. The results are computed thorugh built-in-Shooting method.

The motive of this attempt is explained in three main phase. In first phase, the development of Eyring-Powell nanofluid over a Riga plate in the presence of heat generation, viscus dissipation and chemical reaction with activation energy is elaborated. There is no literature review is presented on such development in the past. In second phase, to demonstrate the impact of different parameters like Prandtl number, Lewis number, Eckert number, thermophoresis and Brownian motion by Riga surface on temperature, velocity and concentration profiles. Finally, to remark the interpretation of Nusselt number, skin friction and Sherwood number which have great importance in industrial characteristics of nanofluids.

2. Mathematical formulation

We take an Eyring-Powell nanofluid flow along a Riga surface under the consideration of the convective boundary conditions for heat and mass transfer. Riga plate is heated with the help of the hot fluid that have an initial temperature $\widetilde{T}_1$ with concentration of particles $\widetilde{C}_{np}$ increases the heat and mass transport of the coefficients $\widetilde{h}_1$ and $\widetilde{h}_2$ respectively. By observing when Lorentz force created by Riga plate as well as the nanoparticles immersion in the fluid then the fluid behaves electrically conducting along *y*-axis. Choose *x*-axis along the surface of the Riga plate and y-axis normal to it. The flow equations in the form of partial differential equations for the presented investigation are given by

$$\frac{\partial \widetilde{u}}{\partial \widetilde{x}} + \frac{\partial \widetilde{v}}{\partial \widetilde{y}} = 0, \tag{1}$$

$$\widetilde{u}\frac{\partial \widetilde{u}}{\partial \widetilde{x}} + \widetilde{v}\frac{\partial \widetilde{u}}{\partial \widetilde{y}} = \left(\widetilde{\nu} + \frac{1}{\widetilde{\rho}_l \widetilde{\gamma}\widetilde{C}^*}\right)\frac{\partial^2 \widetilde{u}}{\partial \widetilde{y}^2} - \frac{1}{2\widetilde{\rho}_l \widetilde{\gamma}\widetilde{C}^{*3}}\left(\frac{\partial \widetilde{u}}{\partial \widetilde{y}}\right)^2 \frac{\partial^2 \widetilde{u}}{\partial \widetilde{y}^2} + \left(\frac{\widetilde{\pi}\widetilde{J}_o.\ \widetilde{M}_o \exp\left(\frac{-\widetilde{\pi}\widetilde{y}}{\widetilde{b}}\right)}{8\widetilde{\rho}_l}\right) - \widetilde{u}\frac{\widetilde{\nu}}{k} - \frac{\widetilde{C}_b}{\sqrt{\widetilde{k}}}\left(\frac{\partial \widetilde{\psi}}{\partial \widetilde{y}}\right)^2, \tag{2}$$

$$\widetilde{u}\frac{\partial \widetilde{T}}{\partial \widetilde{x}} + \widetilde{v}\frac{\partial \widetilde{T}}{\partial \widetilde{y}} = \widetilde{\alpha}\frac{\partial^2 \widetilde{T}}{\partial \widetilde{y}^2} + \widetilde{\tau}\left(\widetilde{D}_B \frac{\partial \widetilde{T}}{\partial \widetilde{y}}\frac{\partial \widetilde{C}}{\partial \widetilde{y}} + \frac{\widetilde{D}_T}{\widetilde{T}_\infty}\left(\frac{\partial \widetilde{T}}{\partial \widetilde{y}}\right)^2\right) + \frac{\widetilde{\nu}}{\widetilde{\rho}\, c_p}\left(\frac{\partial u}{\partial y}\right)^2 - \frac{1}{\widetilde{\rho}\widetilde{c}_p}\frac{\partial \widetilde{q}_r}{\partial \widetilde{y}} + \frac{\widetilde{Q}_0}{\widetilde{\rho}\widetilde{c}_p}(\widetilde{T} - \widetilde{T}_\infty), \tag{3}$$

$$\widetilde{u}\frac{\partial \widetilde{C}}{\partial \widetilde{x}} + \widetilde{v}\frac{\partial \widetilde{C}}{\partial \widetilde{y}} = \widetilde{D}_B\left(\frac{\partial^2 \widetilde{C}}{\partial \widetilde{y}^2}\right) + \frac{\widetilde{D}_T}{\widetilde{T}_\infty}\left(\frac{\partial^2 \widetilde{T}}{\partial \widetilde{y}^2}\right) - \widetilde{K}(\widetilde{C} - \widetilde{C}_\infty) - \widetilde{K}_r^2\left(\frac{\widetilde{T}}{\widetilde{T}_\infty}\right)^n exp\left(\frac{-\widetilde{E}_a}{\widetilde{k}T}\right)(\widetilde{C} - \widetilde{C}_\infty), \tag{4}$$

with the given boundary conditions

$$\tilde{u} = \tilde{x}\tilde{a},\ \tilde{v} = 0,\ -\tilde{k}\frac{\partial \tilde{T}}{\partial \tilde{y}} = \tilde{h}_1^*(\tilde{T}_1 - \tilde{T}),\ -\tilde{D}_B\frac{\partial \tilde{C}}{\partial \tilde{y}} = \tilde{h}_2^*(\tilde{C}_{np} - \tilde{C}) \text{ at } \tilde{y} = 0,$$
$$\tilde{u} \to 0,\ \tilde{T} \to \tilde{T}_\infty,\ \tilde{C} \to \tilde{C}_\infty, \text{ as } \tilde{y} \to \infty \tag{5}$$

By using the concept of Taylor series expansion and Roseland's approximation, we have:

$$q_r = -\frac{4\tilde{\sigma}^*}{3\tilde{k}^*}\frac{\partial \tilde{T}^4}{\partial \tilde{y}^4} \tag{6-a}$$

and

$$\tilde{T}^4 \cong T_\infty^3(4T - 3T_\infty) + \text{Neglecting higher terms} \tag{6-b}$$

So, using eq. (6-b) into (6-a); we get

$$\tilde{q}_r = -\frac{16\tilde{\sigma}^*\tilde{T}_\infty^3}{3\tilde{K}^*}\frac{\partial \tilde{T}}{\partial \tilde{y}} \tag{6-c}$$

With help of Eq. (6-c) in eq. (3) is defined by

$$\tilde{u}\frac{\partial \tilde{T}}{\partial \tilde{x}} + \tilde{v}\frac{\partial \tilde{T}}{\partial \tilde{y}} = \tilde{\alpha}\frac{\partial^2 \tilde{T}}{\partial \tilde{y}^2} + \frac{(\tilde{\rho c})_p}{(\tilde{\rho c})_l}\left(\tilde{D}_B\left(\frac{\partial \tilde{T}}{\partial \tilde{y}}\frac{\partial \tilde{C}}{\partial \tilde{y}}\right) + \frac{\tilde{D}_T}{\tilde{T}_\infty}\left(\frac{\partial \tilde{T}}{\partial \tilde{y}}\right)^2\right) - \frac{\tilde{\nu}}{\tilde{\rho}\tilde{c}_p}\left(\frac{\partial u}{\partial y}\right)^2 + \frac{16\tilde{\sigma}^*\tilde{T}_\infty^3}{3\tilde{K}^*(\tilde{\rho c})_l}\frac{\partial^2 \tilde{T}}{\partial \tilde{y}^2} + \frac{\tilde{Q}_0}{\tilde{\rho}\tilde{c}_p}(T - T_\infty) \tag{7}$$

Introducing the similarity transformation as:

$$\tilde{u} = \frac{\partial \tilde{\psi}}{\partial \tilde{y}},$$
$$\tilde{v} = -\frac{\partial \tilde{\psi}}{\partial \tilde{x}},\ \sqrt{\frac{\tilde{\nu}}{\tilde{a}}}\tilde{\eta} = \tilde{y},\ \frac{\tilde{\psi}}{\tilde{x}\sqrt{\tilde{\nu}\tilde{a}}} = \tilde{f}(\eta)$$
$$\tilde{\theta}(\eta) = \frac{\tilde{T} - \tilde{T}_\infty}{\tilde{T}_1 - \tilde{T}_\infty},\ \tilde{\phi}(\eta) = \frac{\tilde{C} - \tilde{C}_\infty}{\tilde{C}_{np} - \tilde{C}_\infty} \tag{8}$$

Using Eq. (8) into eq. (4, 5) and (7), we get the following nonlinear complex boundary value problem as:

$$\tilde{f}''' + \tilde{K}\tilde{f}''' + \tilde{f}\tilde{f}'' - \tilde{f}'^2 - \tilde{K}\tilde{\Lambda}\tilde{f}''^2\tilde{f}''' + \tilde{Q}\exp(-\tilde{\beta}\tilde{\eta}) - \tilde{D}_1\tilde{f}'(\eta) - \tilde{D}_2\tilde{f}'^2(\eta) = 0 \tag{9}$$

$$\left(1 + \frac{4}{3}\tilde{R}d\right)\tilde{\theta}''(\eta) + \tilde{P}r(\tilde{N}b\tilde{\theta}'(\eta)\tilde{\phi}'(\eta) + \tilde{N}t\tilde{\theta}'^2(\eta) + \tilde{E}c\tilde{f}''^2 + \tilde{q}\tilde{\theta} + \tilde{f}\tilde{\theta}'(\eta)) = 0 \tag{10}$$

$$\tilde{\phi}''(\eta) + \frac{\tilde{N}t}{\tilde{N}b}\tilde{\theta}''(\eta) + \tilde{L}e\tilde{P}r(\tilde{f}\tilde{\phi}'(\eta) - \tilde{K}_1\tilde{\phi}(\eta)) - \tilde{\sigma}(1 + \tilde{\delta}\tilde{\theta})^n exp\left(\frac{-E_a}{k\tilde{T}_\infty(1 + \tilde{\delta}\tilde{\theta})}\right)\tilde{S}c\tilde{\phi} = 0 \tag{11}$$

$$\tilde{f} = 0,\ \frac{\partial \tilde{f}}{\partial \tilde{\eta}} = 1,\ \frac{\partial \tilde{\theta}}{\partial \tilde{\eta}} = -\tilde{\alpha}_1(1 - \tilde{\theta}(0)),\ \frac{\partial \tilde{\phi}}{\partial \tilde{\eta}} = -\tilde{\alpha}_2(1 - \tilde{\phi}(0)) \text{ at } \tilde{\eta} = 0 \tag{12}$$

$$\frac{\partial \tilde{f}}{\partial \tilde{\eta}} \to 0,\ \tilde{\theta} \to 0,\ \tilde{\phi} \to 0, \text{ as } \tilde{\eta} \to \infty \tag{13}$$

Here $\tilde{Q}$ represent the modified Hartman number, $\tilde{P}r$ is used for Prandtl number, $\tilde{R}d$ is known as radiation parameter, $\tilde{\beta}$ is the symbol for dimensionless parameter, $\tilde{N}t$ is used for thermophoresis parameter, $\tilde{N}b$ represent the Brownian motion, $\tilde{K}$ and $\tilde{\Lambda}$ are fluid parameter, $\tilde{\alpha}_1$and $\tilde{\alpha}_2$ are the heat-mass transfer Biot factor, $\tilde{K}_1$ stand for chemical reaction, $\tilde{L}e$ is used for Lewis number, $\tilde{\sigma}$ is used for chemical reaction rate constant, $\tilde{\delta}$ show temperature difference variable, $\tilde{D}_1$and $\tilde{D}_2$is used for non-dimensional porous medium parameters, $\tilde{q}$ is used for heat source/sink, $\tilde{E}c$ is used for Eckert number and $\tilde{S}c$ represented the Schmidt number, respectively. Mathematically, we have the following results

$$\tilde{Q} = \frac{\tilde{\pi}\tilde{J}_o.\tilde{M}_o}{8\tilde{\rho}_l\tilde{x}\tilde{a}^2},\ \tilde{P}r = \frac{\tilde{\nu}}{\tilde{\alpha}},\ \tilde{R}d = \frac{16\tilde{\sigma}^*\tilde{T}_\infty^3}{3\tilde{k}^*\tilde{k}},\ \tilde{\beta} = \frac{\tilde{\pi}}{\tilde{b}}\sqrt{\frac{\tilde{\nu}}{\tilde{a}}},\ \tilde{N}t = \frac{\tilde{\tau}\tilde{D}_T(\tilde{T}_1 - \tilde{T}_\infty)}{\tilde{\nu}\tilde{T}_\infty}$$
$$\tilde{N}b = \frac{\tilde{\tau}\tilde{D}_B(\tilde{C}_{np} - \tilde{C}_\infty)}{\tilde{\nu}},\ \tilde{K} = \frac{1}{\tilde{\mu}\tilde{\gamma}\tilde{C}^*},\ \tilde{\Lambda} = \frac{\tilde{x}^3\tilde{a}^3}{2\tilde{\nu}\tilde{x}\tilde{C}^{*2}},\ \tilde{\alpha}_1 = \frac{\tilde{h}_1^*}{\tilde{k}}\sqrt{\frac{\tilde{\nu}}{\tilde{a}}},\ \tilde{\alpha}_2 = \frac{\tilde{h}_2^*}{\tilde{D}_B}\sqrt{\frac{\tilde{\nu}}{\tilde{a}}}$$
$$\tilde{K}_1 = \frac{\tilde{K}}{\tilde{a}},\ \tilde{L}e = \frac{\tilde{\alpha}}{\tilde{D}_B},\ \tilde{\sigma} = \frac{\tilde{K}_r^2}{\tilde{a}},\ \tilde{\delta} = \frac{\tilde{\theta}(\tilde{T}_1 - \tilde{T}_\infty)}{\tilde{T}_\infty},\ \tilde{D}_1 = \frac{\tilde{\nu}}{\tilde{a}\tilde{k}},\ \tilde{D}_2 = \frac{\tilde{C}_b\tilde{x}}{\sqrt{\tilde{k}}}\ \tilde{q} = \frac{1}{\tilde{a}}\frac{\tilde{Q}_0}{\tilde{\rho}\tilde{c}_p}$$
$$\tilde{E}c = \frac{\tilde{u}^2}{\tilde{\rho}\tilde{c}_p(\tilde{T}_1 - \tilde{T}_\infty)},\ \tilde{S}c = \frac{\tilde{\nu}}{\tilde{D}_B} \tag{14}$$

The important physical quantities namely, Nusselt number (heat flux), Skin-friction (drag force) and Sherwood number (mass flux) are listed below,

$$\tilde{R}\tilde{e}_x^{-1/2}\tilde{N}\tilde{u}_x = -\left(1 + \frac{4}{3}\tilde{R}d\right)\tilde{\theta}'(0)$$
$$\tilde{R}\tilde{e}_x^{-1/2}\tilde{C}_{fx} = \left((1 + \tilde{K})\tilde{f}''(0) - \frac{1}{3}\tilde{K}\tilde{\Lambda}\tilde{f}'^3\right)$$
$$\tilde{R}\tilde{e}_x^{-1/2}\tilde{S}\tilde{h}_x = -\tilde{\phi}'(0) \tag{15}$$

and $\tilde{R}\tilde{e}_x$ presented the local Reynolds number.

3. Results and discussion

This section explore the effects of different immersed parameters and dimensionless numbers on velocity function $f'(\eta)$, temperature function $\theta(\eta)$ and concentration function $\phi(\eta)$ have been discussed. To construct the graphs, we have removed the tilde symbol for the simplicity. We have presented the graphs of velocity, temperature and concentration against the physical parameters. The effects of non-dimensional parameter of porous medium D_1 on velocity field is sketched in Fig. 1. It has a leading impact on the motion of the flow. Ordinarily the defiance in the path of flow is due to porosity, which show the decline behavior of the velocity for the motion of the flow. Actually, for increasing the value of D_1 leads to enhance the number of porous holes which produce defiance in the motion of the flow and decrease the

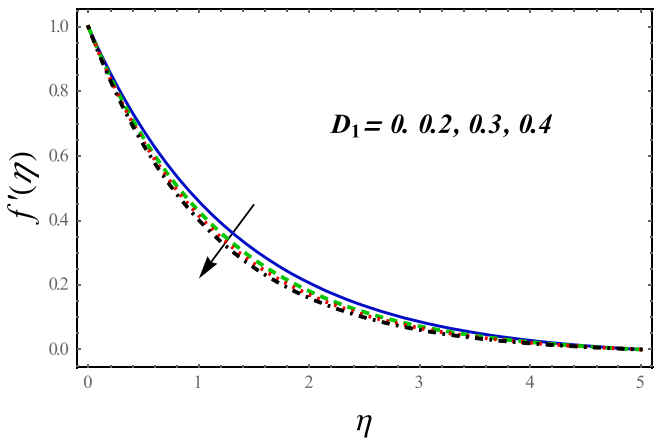

Fig. 1. Impact of D_1 on velocity field.

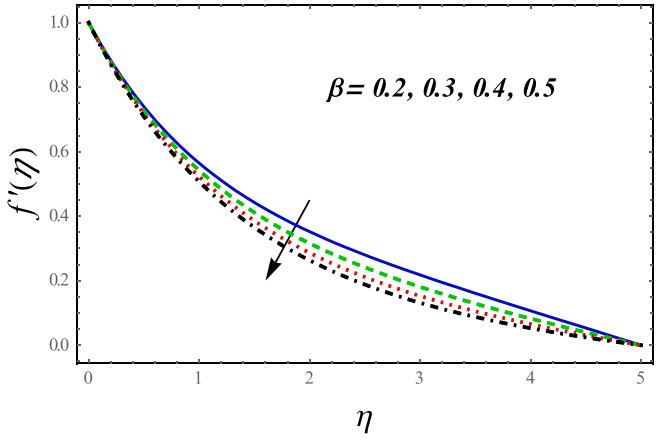

Fig. 2. Impact of β on velocity field.

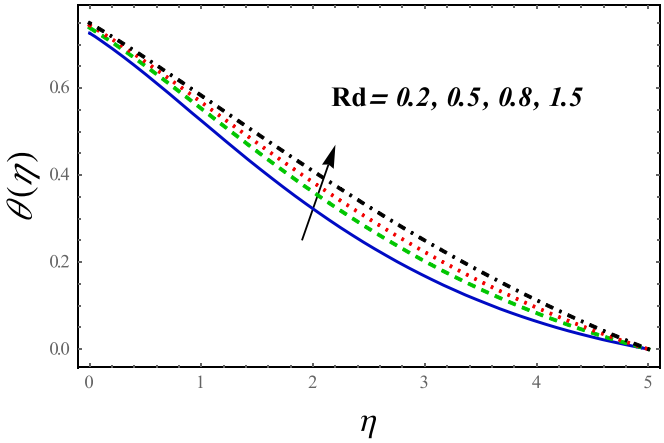

Fig. 5. Impact of Rd on $\theta(\eta)$

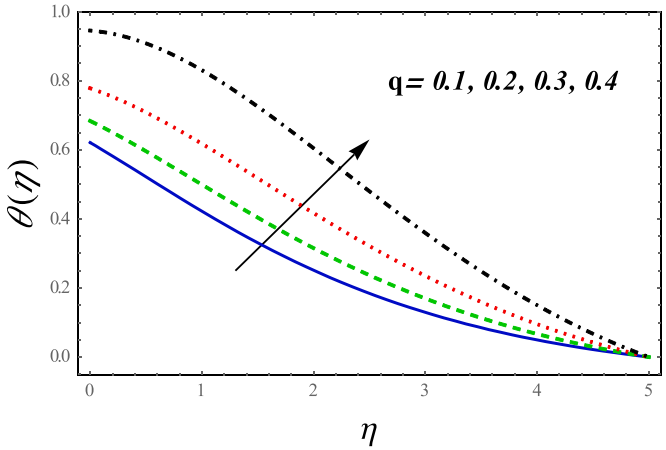

Fig. 3. Impact of q on $\theta(\eta.)$

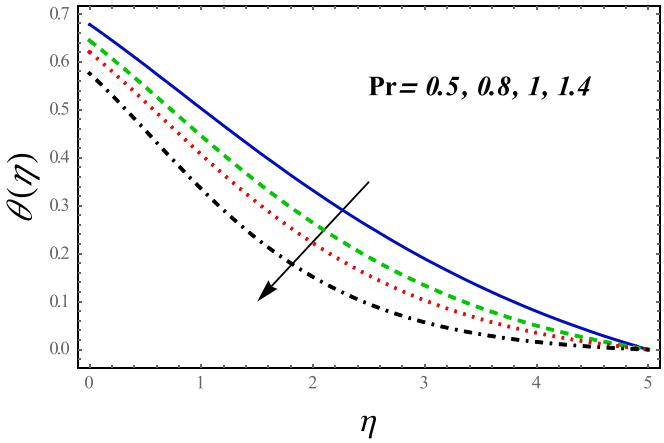

Fig. 6. Impact of Pr on $\theta(\eta)$

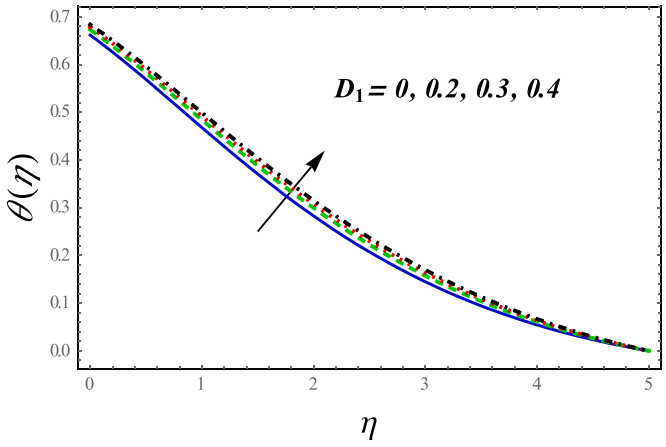

Fig. 4. Impact of D_1 on $\theta(\eta)$

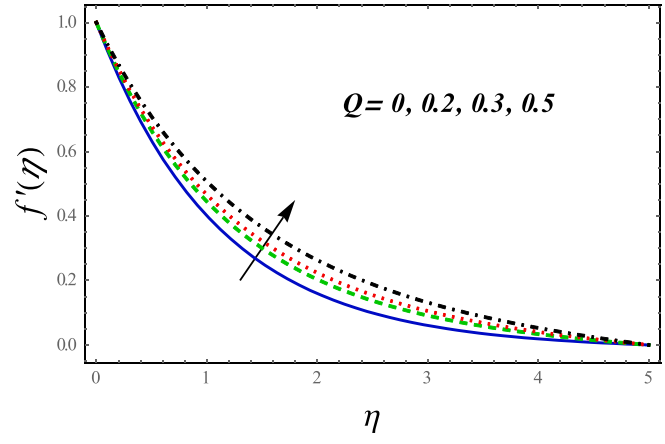

Fig. 7. Impact of Q on velocity field

whole motion of the fluid. Generally, the number of perforations in the porous medium increased with the augmented values of D_1. Passing through these perforations the nanoparticles faced many obstacles. Therefore, it is clear that the velocity profile show decline behavior for the augmented values of D_1. The flow pattern shows decline behavior due to the effect of dimensionless parameter β as illustrated in Fig. 2. Actually, the fluid viscosity increases by the increasing values of β which show the decline behavior of flow pattern. Temperature profile under the action of heat generation/absorption is shown in Fig. 3. Actually the loss of heat for the flow of fluid is due to the heat generation which behaves like a heat generator. The effect of porous medium parameter D_1 on temperature profile is interpreted in Fig. 4. It is noticed that temperature profile showing increasing behavior for the augmented values of porous medium parameter D_1. It is due to the mount of thermal boundary layer that increase with the augmented values of porous medium parameter D_1. The temperature profile under the action of radiation parameter Rd is displayed in Fig. 5. Thermal radiation plays a dominant role in heat transfer for the small value of the convective heat coefficient. The enhancement in the temperature profile is due to the increasing behavior of thermal radiation parameter. This increment

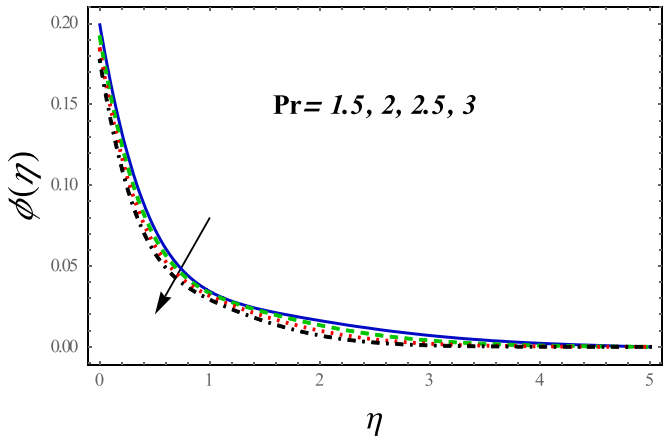

Fig. 8. Impact of *Pr* on $\phi(\eta)$

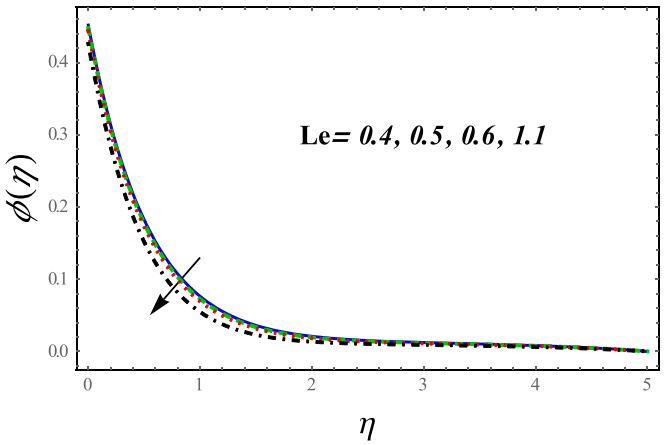

Fig. 11. Impact of *Le* on $\phi(\eta)$

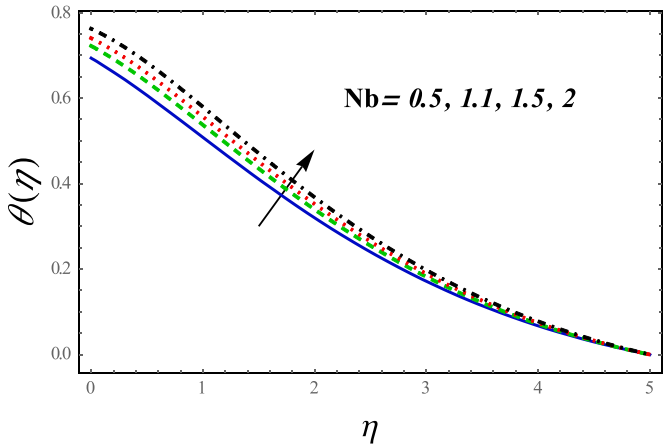

Fig. 9. Impact of Nb on $\theta(\eta)$

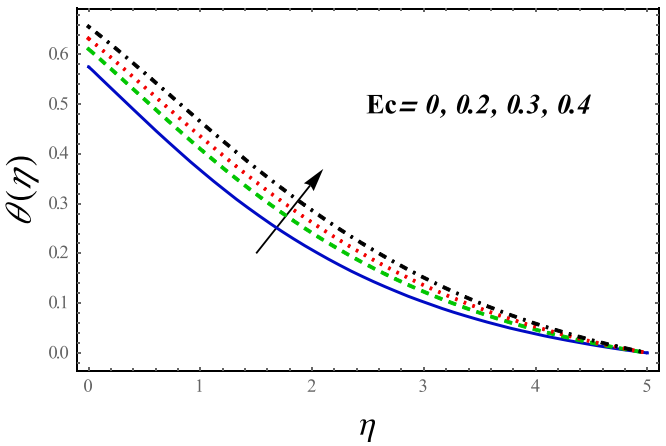

Fig. 12. Impact of Ec on $\theta(\eta)$

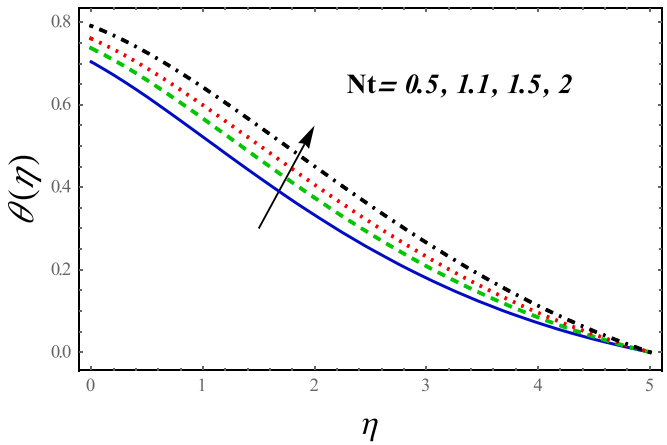

Fig. 10. Impact of Nt on $\theta(\eta)$

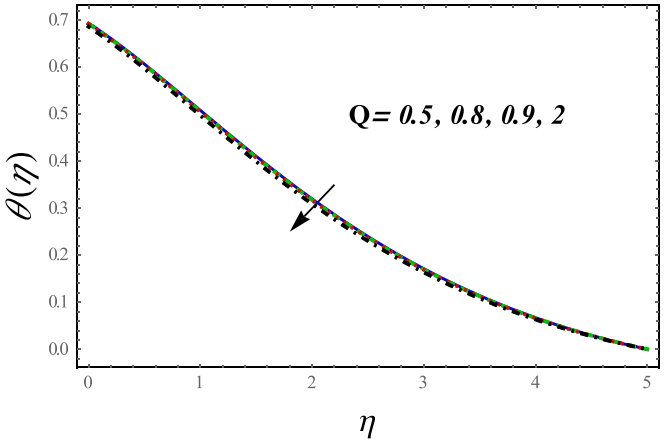

Fig. 13. Impact of Q on $\theta(\eta)$

illustrates the low rate of cooling effect in the flow of nanofluid. The effect of Prandtl number on temperature profile is illustrated in Fig. 6. Substantially, for the low value of *Pr*, the thermal diffusivity is rising behavior for nanofluid but it shows the reverse behavior for higher values of Prandtl number that's why the temperature show decline behavior for liquid. Substantially, *Pr* and thermal diffusivity have inverse relation. Velocity profile under the action of modified Hartman number *Q* is displayed in Fig. 7. It is observed that the velocity shows increasing behavior for the increasing values of modified Hartman number *Q*. Substantially, enhancement in the values of modified Hartman number is show contrasting behavior under the effect of magnetic parameter. Magnetization surrounded by plate, enhanced due to the enhancement in the values of modified Hartman number *Q*, which also help to increase the flow speed of the fluid this is because of magnetic field which is under the action of Lorentz magnetic pull force. This property is completely connected with Riga plate. So, when the modified Hartman number *Q* vanishes the velocities show decline behavior and in this position Riga plate changes into the straight plate. The Prandtl number effect on concentration is displayed in Fig. 8. It is observed that concentration and Prandtl has inverse relation, which

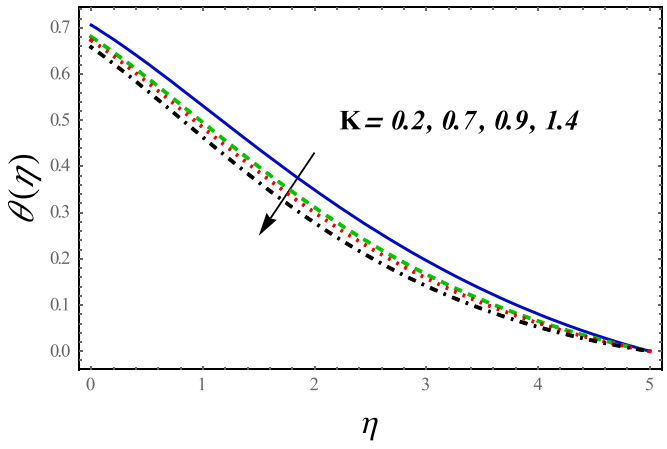

Fig. 14. Impact of K on $\theta(\eta)$

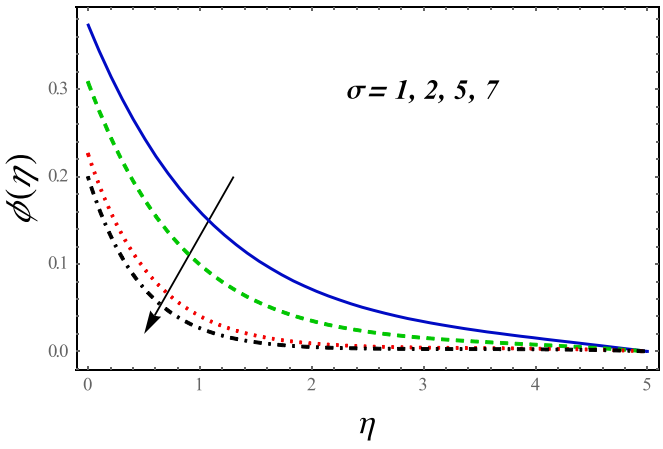

Fig. 17. Impact of σ on $\phi(\eta)$

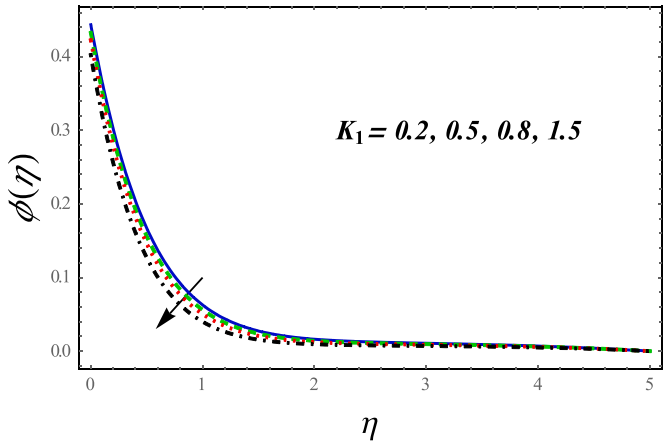

Fig. 15. Impact of K_1 on $\phi(\eta)$

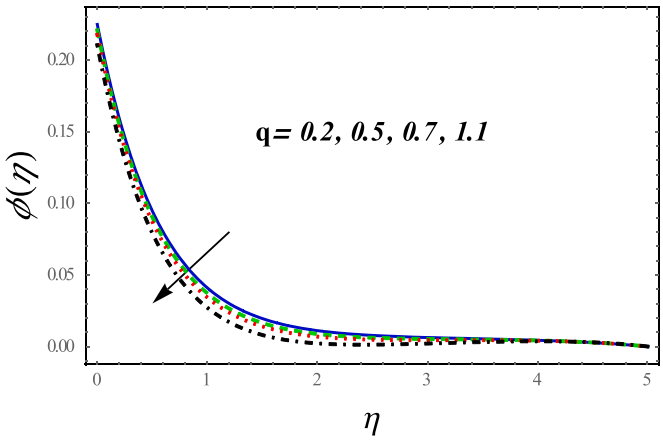

Fig. 18. Impact of q on $\phi(\eta)$

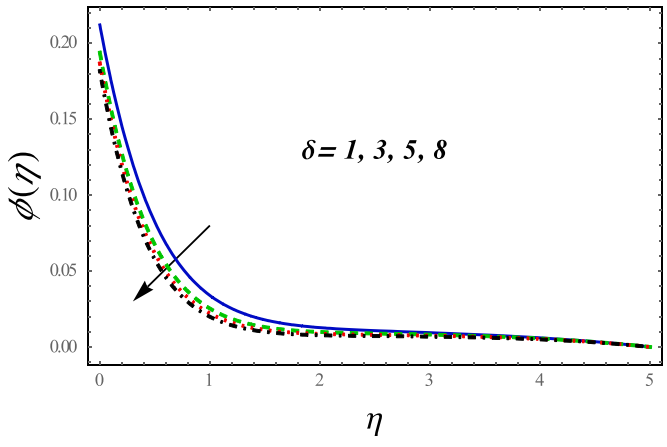

Fig. 16. Impact of δ on $\phi(\eta)$

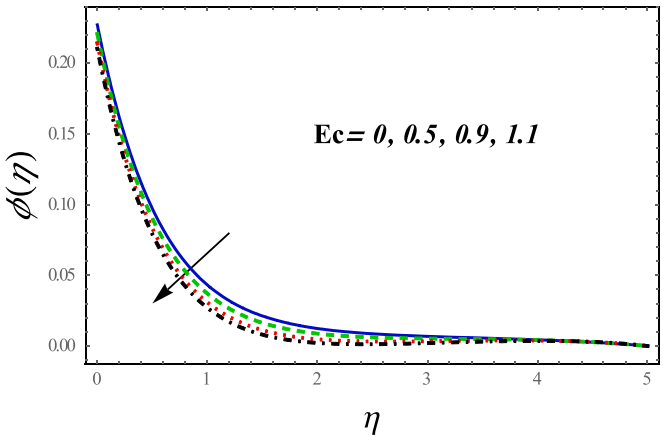

Fig. 19. Impact of Ec on $\phi(\eta)$

show that enhancement in the Prandtl number decreases the concentration profile. Temperature profile under the impact of Brownian motion *Nb* is illustrated in Fig. 9. It is observed that enhancement in the Brownian motion parameter enhance the temperature and also increases the thermal boundary layer thickness. Motion of the particles increases randomly under the action of increasing values of Brownian motion parameter which is the cause of produce more heat. So, temperature profile increases. Observation of thermophoresis effect on temperature profile is displayed in Fig. 10. Increases values of Nt show the leading behavior for both thermal boundary layer thickness and temperature. Thermophoresis is a process in which heated particles moved towards cold place from hot surface, under this behavior temperature of the fluid increases. Analysis of Lewis number on concentration profile is sketched in Fig. 11. For the small values of Lewis number, the concentration profile shows leading behavior. Decline behavior of concentration profile is due to decrease in mass diffusivity which is under the impact of enhancement in the Lewis number. The effect of Eckert number on temperature profile is displayed in Fig. 12. Temperature increase as Eckert number increases because the viscous dissipation increases for the higher values of Eckert Number. Observation of temperature profile under the impact of modified Hartman

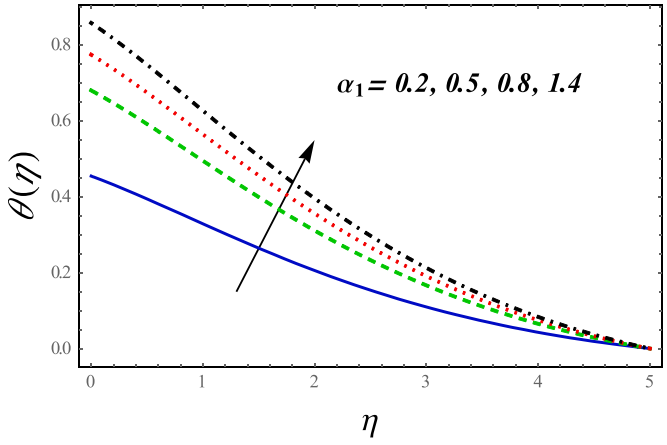

Fig. 20. Impact of α_1 on $\theta(\eta)$

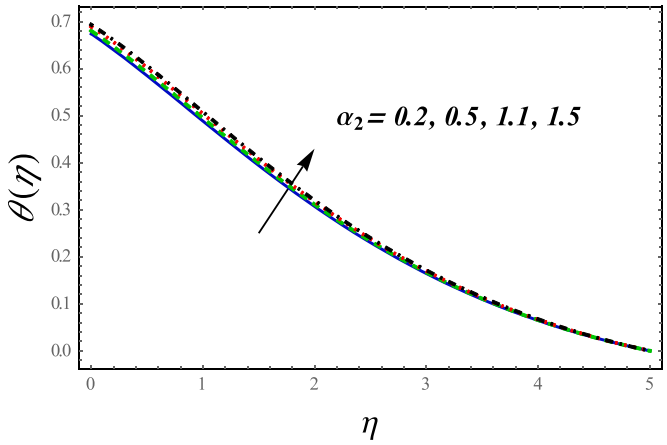

Fig. 21. Impact of α_2 on $\theta(\eta)$

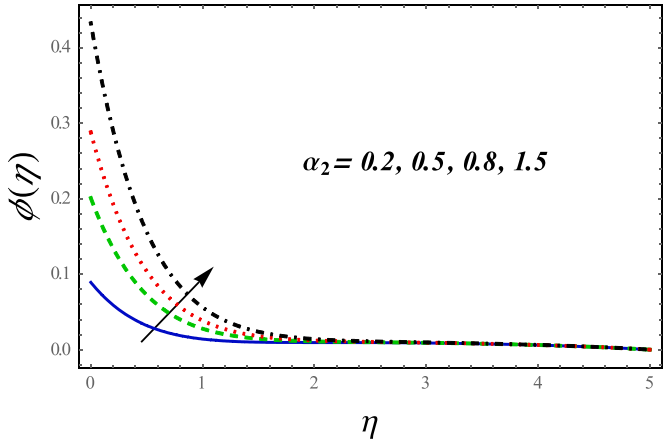

Fig. 22. Impact of α_2 on $\phi(\eta)$

number is elucidated in Fig. 13. The temperature field shows decline behavior for the increasing values of modified Hartman number Q. In the increment of the values of modified Hartman number the thermal boundary layer shows decline behavior. Description of fluid parameter K on the temperature profile is displayed in Fig. 14. It is seen that for the fluid parameter K temperature profile show decline behavior. Because the augmented values of K reduce the dynamic viscosity which result in decreasing the temperature profile. Fig. 15 reported the impact of chemical reaction on the concentration profile. It is observed that concentration profile reduces for the augmented values of chemical

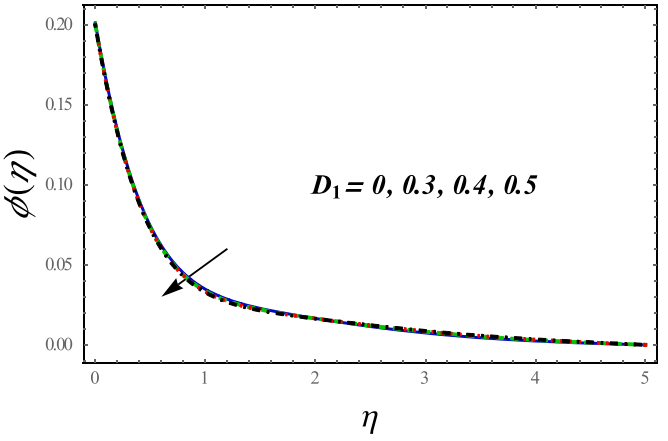

Fig. 23. Impact of D_1 on $\phi(\eta)$

Table 1
Variation of Drag force via non-dimensional parameters.

$\widetilde{\beta}$	$\widetilde{K}$	$\widetilde{Q}$	$\widetilde{R}\widetilde{e}_x^{-1/2}\widetilde{C}_{fx}$
0.0	0.3	0.3	0.9282
0.5			0.9909
1.0			1.0267
1.1	0.0	0.3	1.1434
	0.5		0.9723
	1.0		0.8592
1.1	0.3	0.0	1.1412
		0.5	0.9607
		1.0	0.7866

Table 2
Variation of Nusselt number and Sherwood number via non-dimensional parameters.

$\widetilde{D}_1$	$\widetilde{q}$	$\widetilde{E}c$	$\widetilde{P}r$	$\widetilde{R}d$	$\widetilde{R}\widetilde{e}_x^{-1/2}\widetilde{N}\widetilde{u}_x$	$\widetilde{R}\widetilde{e}_x^{-1/2}\widetilde{S}\widetilde{h}_x$
0.2	0.3	0.4	0.5	0.3	0.7914	0.2120
		0.5			0.8003	0.2104
		0.6			0.8095	0.2088
0.2	0.1	0.2	0.5	0.3	0.7639	0.2171
	0.2				0.7691	0.2162
	0.4				0.7800	0.2141
0.3	0.5	0.2	0.5	0.3	0.7876	0.2130
0.4					0.7895	0.2128
0.5					0.7913	0.2127
0.6	0.5	0.2	0.6	0.3	0.7837	0.2087
			0.7		0.7744	0.2050
			0.8		0.7654	0.2015
0.6	0.5	0.2	0.9	0.4	0.8360	0.1980
				0.5	0.9156	0.1978
				0.6	0.9954	0.1977

reaction due to riddling between the particles of the fluid towards the surface increases for the augmented values of K_1 which leads to decrease the corresponding boundary layer. The characteristics of temperature difference parameter δ and chemical reaction rate constant σ on concentration profile $\phi(\eta)$ is elaborated in Figs. 16 and 17, respectively. We analyzed that for different values δ and σ concentration profile shows decline behavior. Because the rate of destructive chemical reaction increases. In Fig. 18, we observed that an enhancement in heat source parameter q reduce the nanoparticles concentration $\phi(\eta)$. This occurs under the impact of the boundary layer thickness gain energy from the thermal boundary layer as a result reduce the concentration profile. Concentration profile under the impact of Eckert number is displayed in Fig. 19. We analyzed that an increment in the values of Eckert number decreases the concentration profile. Temperature profile

under the impact of $\alpha_1$is demonstrated in Fig. 20. Stronger convection creates due to the augmented values of $\alpha_1$which result in raising behavior of temperature profile. It is due to the related boundary layer mount for the augmented values of α_1. Descriptive of α_2 on temperature profile is elaborated in Fig. 21. Mass convection increased by an increment in the values of α_2. This augmented conclusion in arise of the identical boundary layer and temperature profile. Impact of α_2 on concentration profile is elucidated in Fig. 22. The concentration profile enhanced for the augmented values of α_2. Mass convection is connected to the Biot factor. Augmented values of concentration profile is due to the stronger mass Biot factor. Non-dimensional porous medium parameter D_1 effect on concentration profile is subjected in Fig. 23. It is noticed that for the augmented values of non-dimensional porous medium parameter the concentration profile show rising behavior. It is due to an increment in the values of the non-dimensional porous medium parameter that increases the thickness of the solutal boundary layer. Substantially, it is elaborated as enhancement in the non-dimensional porous medium parameter gives more spaces for the entrance of heat in the flow of the fluid. The numerical values of important physical quantities are listed in Table 1. It is observed that the drag-force is increases for increasing the values of β while an reverse trend is observed against $\widetilde{K}$ and $\widetilde{Q}$.

The obtaining results for Sherwood numbers and Nusselt number for different pertinent parameters are displayed in Table 2. From this table it is noted that the values of heat transfer rate showing the increasing trend via D_1, $\widetilde{q}$, $\widetilde{E}c$ and Rd while opposite behavior is observed via $\widetilde{P}r$. Moreover, the values of Sherwood number predicting the decreasing behavior via D_1, $\widetilde{q}$, $\widetilde{E}c$, $Rd\,\widetilde{q}$ and $\widetilde{E}c$.

4. Conclusions

In this study we explored the effects of activation energy, thermal radiation, heat generation, porous medium and chemical reaction on Eyring-Powell nanofluid flow along the Riga surface. The set of partial differential equations are converted into ordinary differential equation by using the suitable similarity transformation and solved them numerically. The concluding note about this study are elaborated below:

- For the augmented values of porous medium parameter and magnetic field the velocity decreases.
- The temperature profiles accelerate against the Prandlt number while an opposite trend is observed via heat generation and radiation parameters.
- Temperature and concentration profiles show decline behavior for the augmented values of fluid parameter.
- For an increasing values of modified Hartman number temperature show decline behavior.
- Eckert number declines the temperature and nanoparticles concentration profiles.
- For an increasing values of heat source parameter $q > 0$ temperature show raising behavior but for heat sink parameter $q < 0$ it show decline behavior.
- Sherwood number predicting the decreasing behavior via D_1, $\widetilde{q}$, $\widetilde{E}c$, $Rd\,\widetilde{q}$ and $\widetilde{E}c$.

Declaration of Competing Interest

The authors declare that they have no known competing financial interests or personal relationships that could have appeared to influence the work reported in this paper.

References

[1] S. Choi, J. Eastman, Enhancing thermal conductivity of fluids with nanoparticles, Enhancing Thermal Conduct. Fluids Nanoparticles 2 (1) (1995) 99–105.
[2] G. Rasool, T. Zhang, Characteristics of chemical reaction and convective boundary conditions in Powell-Eyring nanofluid flow along a radiative Riga plate, Heliyon 5 (4) (2019) e01479.
[3] J. Buongiorno, Convective transport in nanofluids, J. Heat Transf. 128 (3) (2006) 240–250.
[4] M. Sheikholeslami, G. Bandpy, R. Ellahi, M. Hassan, S. Soleimani, Effects of MHD on cu-water nanofluid flow and heat transfer by means of CVFEM, J. Magn. Magn. Mater. 349 (1) (2014) 188–200.
[5] M. Turkyilmazoglu, Exact analytical solutions for heat and mass transfer of MHD slip flow in nanofluids, Chem. Eng. Sci. 84 (2) (2012) 182–187.
[6] T. Hayat, T. Muhammad, A. Alsaedi, M. Alhuthali, Magneto-hydrodynamic three-dimensional flow of viscoelastic nanofluid in the presence of nonlinear thermal radiation, J. Magn. Magn. Mater. 385 (1) (2015) 222–229.
[7] T. Hayat, T. Muhammad, M. Shehzad, G. Chen, I. Abbas, Interaction of magnetic field in flow of Maxwell nanofluid with convective effect, J. Magn. Magn. Mater. 389 (1) (2015) 48–55.
[8] A. Chamkha, S. Abbasbandy, A. Rashad, Non-Darcy natural convection flow for non-Newtonian nanofluid over cone saturated in porous medium with uniform heat and volume fraction fluxes, Int. J. Num. Met. Heat Fluid Flow 25 (2) (2015) 422–437.
[9] A. Zeeshan, A. Majeed, R. Ellahi, Effect of magnetic dipole on viscous ferro-fluid past a stretching surface with thermal radiation, J. Mol. Liq. 215 (1) (2016) 549–554.
[10] T. Mustafa, Buongiorno model in a nanofluid filled asymmetric channel fulfilling zero net particle flux at the walls, Int. J. Heat Mass Transf. 126 (1) (2018) 974–979.
[11] M. Waqas, S. Jabeen, T. Hayat, S. Shehzad, A. Alsaedi, Numerical simulation for nonlinear radiated Eyring-Powell nanofluid considering magnetic dipole and activation energy, Int. Commun. Heat Mass Transfer 112 (1) (2020) 104401.
[12] A. Gailitis, O. Lielausis, On a possibility to reduce the hydrodynamic resistance of a plate in an electrolyte, Appl. Mag. Rep. Phys. Inst 12 (1) (1961) 143–146.
[13] E. Magyari, A. Pantokratoras, Aiding and opposing mixed convection flows over the Riga-plate, Commun. Nonlinear Sci. Numer. Simul. 16 (8) (2011) 3158–3167.
[14] M. Sheikholeslami, A. Chamkha, Influence of Lorentz forces on nanofluid forced convection considering Marangoni convection, J. Mol. Liq. 225 (1) (2017) 750–757.
[15] N. Balazadeh, M. Sheikholeslami, D. Ganji, Li Zhixiong, Semi analytical analysis for transient Eyring-Powell squeezing flow in a stretching channel due to magnetic field using DTM, J. Mol. Liq. 260 (1) (2018) 30–36.
[16] S. Seyed, B. Saray, A. Chamkha, Heat and mass transfer investigation of magneto-hydrodynamic Eyring-Powell flow in a stretching channel with chemical reactions, Phys. A Statis. Mech. Appl. 554 (2) (2020) 124109.
[17] A. Khan, Effects of homogeneous–heterogeneous reactions on the viscoelastic fluid toward a stretching sheet, J. Heat Transf. 134 (6) (2012) 064506.
[18] T. Hayat, M. Khan, M. Imtiaz, A. Alsaedi, Squeezing flow past a Riga plate with chemical reaction and convective conditions, J. Mol. Liq. 225 (1) (2017) 569–576.
[19] N. Ali, F. Nazeer, Mubbashar Nazeer flow and heat transfer of Eyring-Powell fluid in a pipe, Zeitschrift für Naturforschung A (ZNA) 73 (3) (2018) 265–274.
[20] A. Alsaedi, T. Hayat, Q. Qayyum, R. Yaqoob, Eyring–Powell nanofluid flow with nonlinear mixed convection: entropy generation minimization, Comput. Methods Prog. Biomed. 186 (1) (2020) 105183.
[21] Mubbashar Nazeer, Fayyaz Ahmed, Adila Saleem, Mubashara Saeed, Sidra Naveed, Mubarra Shaheen, Eman Al Aidarous, Effects of constant and space dependent viscosity on Eyring-Powell fluid in a pipe: comparison of perturbation and explicit finite difference method, Zeitschrift für Naturforschung A (ZNA) 74 (2019) 11)a, 961–969.
[22] Mubbashar Nazeer, Fayyaz Ahmed, Mubashara Saeed, Adila Saleem, Sidra Naveed, Zeeshan Akram, Numerical solution for flow of a Eyring-Powell fluid in a pipe with prescribed surface temperature, J. Braz. Soc. Mech. Sci. Eng. 41 (2019) 518.
[23] Fayyaz Ahmed, Mubbashar Nazeer, Mubashara Saeed, Adila Saleem, Waqas Ali, Heat and mass transfer of temperature-dependent viscosity models in a pipe: effects of thermal radiation and heat generation, Zeitschrift für Naturforschung A (ZNA) 75 ((3)a) (2020) 225–239.
[24] M.I Khan, M. Waqas, T. Hayat, A. Alsaedi, A comparative study of Casson fluid with homogeneous-heterogeneous reactions, J. Colloid Interface Sci. 498 (2017) 85–90.